Tikrit Journal of Pure Science Vol. 30 (5) 2025

DOI: *https://doi.org/10.25130/tjps.v30i6.1871*

IRAQI Academic Scientific Journals

Tikrit Journal of Pure Science

ISSN: 1813 – 1662 (Print) --- E-ISSN: 2415 – 1726 (Online)

Journal Homepage: https://tjpsj.org/

Design of Dual Band Microstrip Antenna Planner Array (1×2) for Wireless Applications

Heba Ahmed Abu Al-Yaqdan[1], **Faris Saleh Atallah**[2]

[1,2]*Department of Physics, College of Science, University of Tikrit, Tikrit, Iraq*

Received: 8 Jan. 2025 **Received in revised forum:** 12 Feb. 2025 **Accepted:** 18 Feb. 2025

Final Proofreading: 22 Apr. 2025 **Available online:** 25 Dec. 2025

ABSTRACT

In this research, a (1x2) microstrip antenna array operating over a wide frequency range (3.564 – 8.796 GHz) has been designed, making it suitable for wireless communication applications such as WiMAX, WLAN, and emerging 5 G systems. The design was simulated using computer simulation technology (CST) Studio Suite 2021. The antenna employs a microstrip-line feeding technique, a direct feeding method. This technique is characterized by its ease of fabrication and substrate etching. Copper was used to design both the ground plane and the radiating patch, separated by an FR-4 lossy substrate with a dielectric constant of 4.3 and a thickness of 1.6 mm. The overall dimensions of the antenna are (85 × 38 × 1.6 mm). The results gained at the first frequency (3.564 GHz) are (4.670664 dB), and at the second frequency (8.796 GHz), they are (2.4549 dB). The directivity at the first frequency is (4.242 dB), and at the second frequency is (5.7148 dB). The efficiency at the first frequency is (86.9077 %), and at the second frequency it is (89.2244 %). The bandwidth at the first frequency is (0.7209 GHz), and at the second frequency, it is (0.5071 GHz). The return loss at the first frequency is (- -32.3959 dB), and at the second frequency, it is (- -32.0718 dB). At the first frequency, the voltage standing wave ratio is (1.0559), and at the second frequency, it is (1.0530). The current distribution at the first frequency is (43.2488 A/m), and at the second frequency, it is (46.8896 A/m). The results show that the design supports the wireless communication applications targeted in the research and is highly efficient.

Keywords: Gain, Directivity, Efficiency, Return Loss, Voltage Standing Wave, Current Distribution.

Name: **Heba Ahmed Abu Al-Yaqdan** **E-mail:** Reemtyu863@gmail.com

Tikrit Journal of Pure Science Vol. 30 (5) 2025
DOI: https://doi.org/10.25130/tjps.v30i6.1871

تصميم مصفوفة هوائي الشريحة الرقيقة ثنائي النطاق (2×1) لتطبيقات الاتصالات اللاسلكية

هبه احمد ابو اليقضان، فارس صالح عطاالله

قسم الفيزياء، كلية العلوم، جامعة تكريت، تكريت، العراق

الملخص

في هذا البحث تم تصميم مصفوفة هوائي الشريحة الرقيقة (2×1) تعمل عند نطاق ترددي واسع (3.564 – 8.796 GHz) مما يجعلها مناسبة لتطبيقات الاتصالات اللاسلكية (WiMAX, WLAN) تم التصميم باستخدام برنامج المحاكاة (CST 2021) تم استخدام تقنية التغذية الخط الشريطي وهي احدى تقنيات تغذية الهوائي المباشرة الاتصال بخط النقل وتتميز بسهولة تصنيعها وحفرها على الركيزة واستعمال مادة النحاس لتصميم المستوى الارضي والرقعة المشعة وتفصل بينهما الركيزة (FR-4 loss) ذات ثابت عزل (4.3) وبسُمك (1.6 mm) وبأبعاد كلية (85 × 38 × 1.6 mm) حيث اظهرت النتائج الكسب عند التردد الاول (3.564 GHz) تساوي (4.670664 dB) والتردد الثاني (8.796 GHz) تساوي (2.4549 dB) الاتجاهية عند التردد الاول تساوي (4.242 dB) والتردد الثاني تساوي (5.7148 dB) والكفاءة عند التردد الاول تساوي (86.9077 %) والتردد الثاني تساوي (89.2244 %) وعرض النطاق الترددي عند التردد الاول تساوي (0.7209 GHz) بينما عند التردد الثاني تساوي (0.5071 GHz) وجد ان خسارة العودة عند التردد الاول تساوي (-32.3959 dB) بينما عند التردد الثاني تساوي (-32.0718 dB) وان فولتية الموجة الواقفة عند التردد الاول تساوي (1.0559) بينما عند التردد الثاني تساوي (1.0530) وتوزيع التيار عند التردد الاول يساوي (43.2488 A/m). بينما عند التردد الثاني يساوي (46.8896 A/m) وتبين من النتائج ان التصميم يدعم التطبيقات الاتصالات اللاسلكية المستهدفة في البحث و ذو كفاءة عالية.

INTRODUCTION

Antennas have become increasingly important to our society; they are now indispensable. An electromagnetic transducer, called an antenna, is used to convert guided waves in transmission lines into freely propagating waves, and vice versa. The history of the antenna dates back to James Maxwell, who represented and unified the theories of magnetism and electricity. Maxwell's equations, which describe these relationships, were first published in 1873. When the electromagnetic field produced by the source is transmitted to the antenna system via a transmission line and subsequently radiated into free space, this is known as antenna radiation [1, 2]. The fundamental principle behind all antennas is that radiation is emitted by electric charges that accelerate (either speeding up or slowing down) [3, 4]. Microstrip antennas are among the most important types of antennas and are preferred in antenna design. The antenna is a very thin metallic microstrip, typically made of copper or gold, placed above a ground plane [5]. A dielectric layer, the substrate, separates the strip and the ground plane (representing the patch). The patch can take various shapes, such as rectangular, circular, and others. These antennas are characterized by being lightweight, compact, low-cost, and capable of efficient mass production. Because they offer better radiation characteristics, including gain, directivity, a lower voltage standing wave ratio (VSWR), and reduced return loss, microstrip antenna arrays stand out among other microstrip antenna designs. Applications for them are numerous across various wireless communication systems. Figure 1 shows a microstrip antenna array[6].

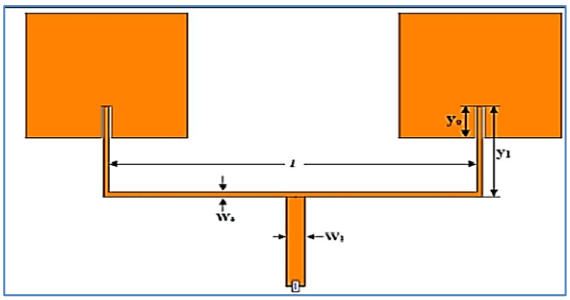

Fig. 1: Geometrical scheme of (1×2) Microstrip antenna array (6).

MATERIALS AND METHODS

The computer simulation software CST 2021 was used to design a (1×2) array and a printed circuit board (PCB), an electronic board used in the manufacturing of electronic circuits, such as antennas. The PCB consists of three layers, including two copper layers and an FR-4 substrate with a dielectric constant of 4.3 and a thickness of 1.6 mm. FR-4 was selected due to its widespread availability, low cost, ease of fabrication, and proven suitability for multi-band wireless communication applications within the specified frequency range (3.564 - 8.796 GHz). This choice addresses potential concerns about material performance and sourcing, especially in local manufacturing contexts, avoiding the need for expensive or hard-to-source materials like R04003C. An antenna array is a set of antennas that radiate in all directions, where each antenna sends the same signal, and the resulting waves experience destructive and constructive interference. The array was properly placed and built, and the elements were arranged with a distance equal to (lambda over 2) between them. Where λ is the wavelength. The design of a microstrip antenna array (1×2) was completed using the simulation software CST-2021. The epoxy material FR-4 Loss was used as the dielectric substrate with a relative permittivity of (1.6 mm) and substrate dielectric constant (ε_r = 4.3). The operating frequency range is between (3.564 and 8.796 GHz), which is suitable for wireless applications such as (WiMAX – WLAN). Copper was used as the conductive material for both the patch and the ground plane, and a microstrip feeding technique was applied. Several mathematical formulas were used to calculate the primary dimensions of the patch to obtain correct values for the length and width of the rectangular patch as follows:

The patch's width (W_p) was calculated by the equation (1), and the result was (W_P = 26 mm) [7].

$$W_P = \frac{C_o}{F}\sqrt{\frac{2}{\varepsilon_r+1}} \quad \ldots (1)$$

W_P Is the patch's width, C is the velocity of light, F is the frequency of resonance, and ε_r It is the dielectric constant. The length of the patch (L_p) was calculated by equation (2), and the result was (L_P = 30.1716 mm)[8].

$$L_P = L_{eff} - 2\Delta L \quad \ldots (2)$$

ΔL is the distinction between electrical and physical lengths and L_{eff} Is the effective length of the patch. Figure 2 shows the transmission line [8].

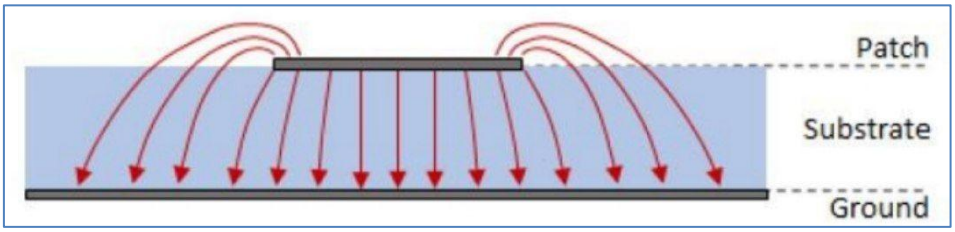

Fig. 2. Transmission line (8).

The effective length of the patch (L_{eff}) was found by using equation (3), and the result was (L_{eff}= 31.644 mm)[9].

$$L_{eff} = \frac{c}{2f_r\sqrt{\varepsilon_{erff}}} \quad \ldots (3)$$

The effective dielectric constant (ε_{reff}) was calculated using equation (4), and the result was (ε_{reff} = 3.901)[10].

$$\varepsilon_{reff} = \frac{\varepsilon_r+1}{2} + \frac{\varepsilon_r-1}{2}\left(\frac{1}{\sqrt{1+\frac{12h}{W_p}}}\right) \quad \ldots (4)$$

The Equation was used to determine the difference between the patch's electrical and physical lengths (5), and the result was (ΔL = 0.7362 mm) [11].

$$\frac{\Delta L}{h} = 0.412\left[\frac{(\varepsilon_{reff}+0.3)\left(\frac{W_p+0.264}{h}\right)}{(\varepsilon_{reff}-0.258)\left(\frac{W_p}{h}+0.8\right)}\right] \quad \ldots (5)$$

The proposed microstrip antenna array (1×2) is shown in Figure 3, and the details of the proposed microstrip antenna array (1×2) are shown in Table 1.

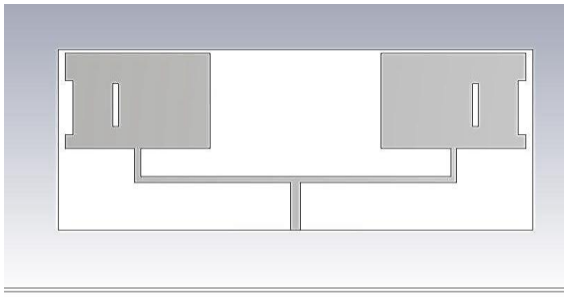

Fig. 3: The proposed microstrip antenna array (1×2).

Table (1): Details of the proposed microstrip antenna array (1×2).

Parameter	Description	Value
Ws	width of substrate	85(mm)
Ls	Substrate's length	38 (mm)
Wp	width of the patch	26 (mm)
Lp	length of the patch	20 (mm)
Wf	width of the feed line	1.8 (mm)
Lf	Transmission line length	10 (mm)
S	Strip feed line width S	6 (mm)
R	Feed line display for the first branch in the array antenna	1.1 (mm)
ε_r	Dielectric constant	4.3
T	Thickness of the patch	0.035 (mm)
H	Substrate thickness	1.6 (mm)
F	Resonant frequency	3.564 – 8.796 (GHz)
N	The dimensions of the center slot	1.80 (mm)

RESULTS AND DISCUSSION

As shown in Figure 4, the microstrip line feeds the gain of the microstrip antenna array. At a frequency of (3.564 GHz), it is equal to (4.670664 dB), and at a frequency of (8.796 GHz), it is (2.45404 dB). The proposed antenna delivers superior gain, enhancing signal strength and coverage. The following mathematical formula (6)[12, 13].

$$G=4\pi\left(\frac{U(\theta,\varphi)}{P_{in}}\right) \quad \ldots (6)$$

G Is the gain, $U(\theta,\varphi)$ Is the radiation intensity in a specific direction, and P_{in} Is the antenna input power?

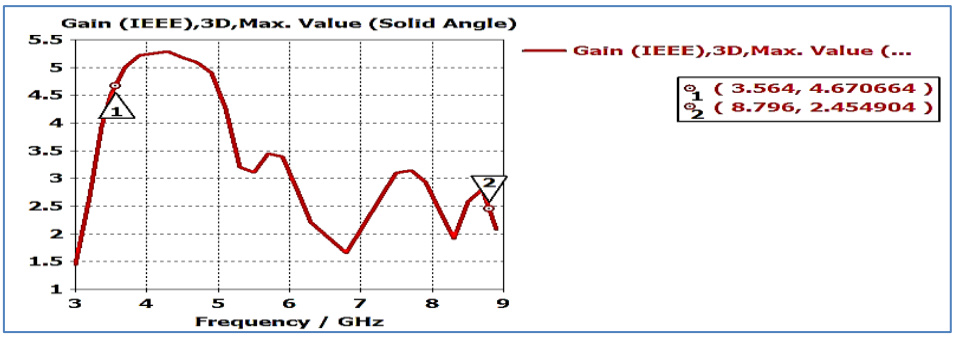

Fig. 4: Gain as a function of frequency.

Figure 5 shows directivity as a function of frequency. The simulation results using CST showed that the directivity at frequency (3.564 GHz) was equal to (5.765766 dB), while at frequency (8.796 GHz) it was equal to (6.16404 dB), which was calculated using the mathematical equation (7)[14, 15].

$$D=4\pi\frac{U_{max}}{P_{rad}} \quad \dots (7)$$

D Is the directivity, U_{max} is the peak radiation intensity, and P_{rad} Is the radiant power. The proposed microstrip antenna array exhibits exceptional directivity, enabling precise radiation concentration in a targeted direction. This enhanced directional capability significantly improves transmission and reception efficiency while minimizing interference from extraneous signals. Consequently, the microstrip antenna's performance is optimized, ensuring superior signal strength and coverage in the desired areas.

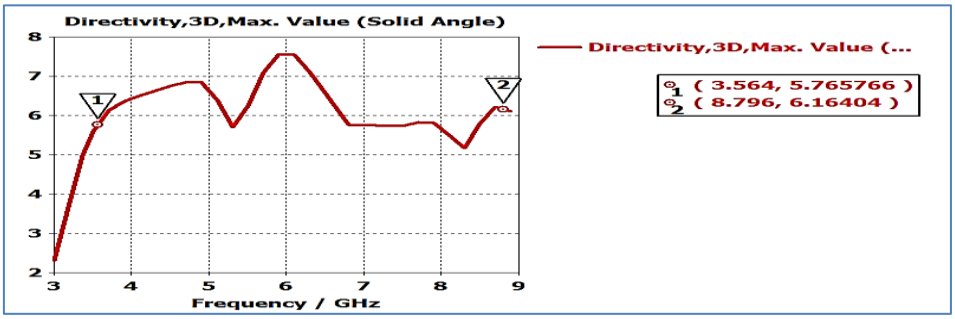

Fig. 5: Directivity as a function of frequency

The Efficiency of the microstrip antenna array (1×2) simulation results from (CST) showed that the efficiency at frequency (3.564 GHz) was (86.9077 %), while at frequency (8.796 GHz) it was (89.2244 %), by equation (8)[16]. The high radiation efficiency confirms minimal losses and optimal performance.

$$\eta=\frac{G}{D}x100 \quad \dots (8)$$

η is the efficiency, G is the gain, and D is the directivity. Figure 6 shows the return loss. Simulation results from CST showed that the return loss at a frequency of (3.564 GHz) was (- -32.07171 dB), while at a frequency of (8.796 GHz) it was (- -32.3959 dB). The lower the return loss, typically below a specified threshold (-10 dB), the better the antenna's performance in transmitting electromagnetic energy into the medium without significant energy loss. The low return loss signifies excellent impedance matching and minimal reflection. It is given by equation (9) [17, 18].

$$RL(dB)=10\ \log\frac{p_{ref}}{p_{in}} \quad \dots (9)$$

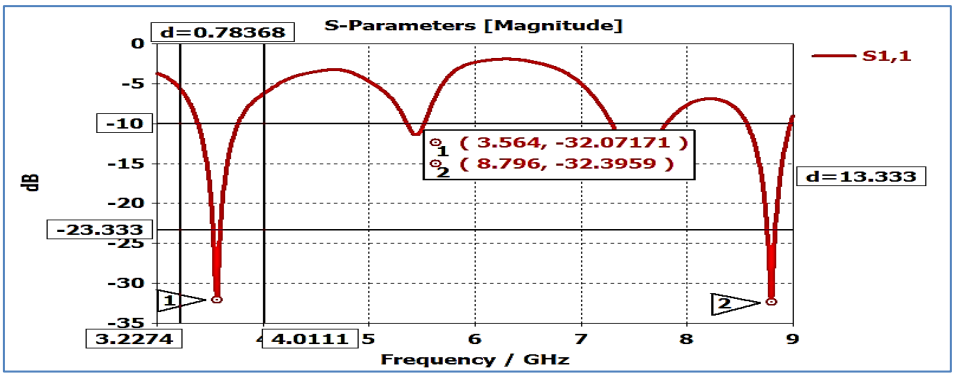

Fig. 6: Return loss as a function of frequency

Figure 7 shows the voltage standing wave ratio. The simulation results in CST showed that at a frequency of (3.564 GHz), it equals (1.051098). A VSWR close to unity validates the microstrip antenna array's near-ideal impedance matching.

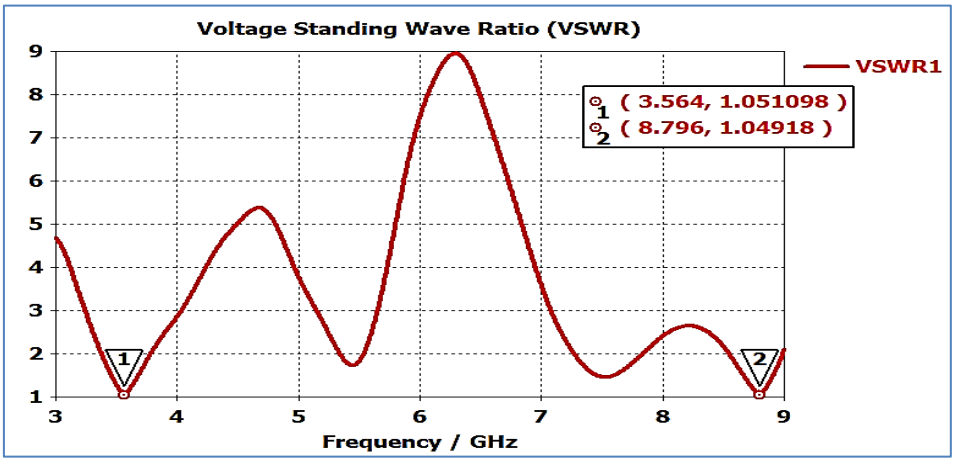

Fig. 7: Voltage Standing Wave Ratio as a function of frequency

Figure 8 shows the current distribution. The red areas indicate the current distribution zones. The simulation results in CST showed that at a frequency of (3.564 GHz) it equals (35.0659 A/m) as shown in the figure (8-a), while at a frequency of (8.796 GHz) it equals (32.8056 A/m) as shown in the figure (8-b).

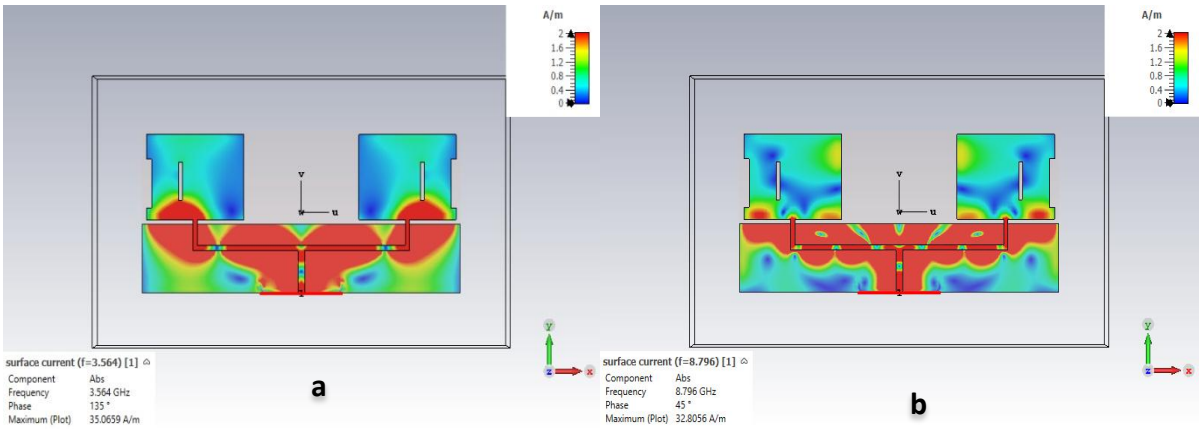

Fig. 8: Current distribution as a function of frequency: (a) Low-frequency range, (b) High-frequency range.

Figure 9 illustrates the radiation pattern obtained from simulations conducted with CST-2021. The results depict the radiation patterns of both the electric and magnetic fields for a (1×2) microstrip antenna array operating within the frequency range of (3.564 to 8.796 GHz). These patterns are presented as a function of frequency. The horizontal plane (X-Z) corresponds to the electric field (E-Plane), while the vertical plane (Y-Z) represents the magnetic field (H-Plane). The E-Plane is calculated at an azimuthal angle of (Phi = 0°), whereas the H-Plane is calculated at an azimuthal angle of (Phi = 90°). This analysis provides a comprehensive understanding of the directional characteristics and electromagnetic field distribution of the microstrip antenna array.

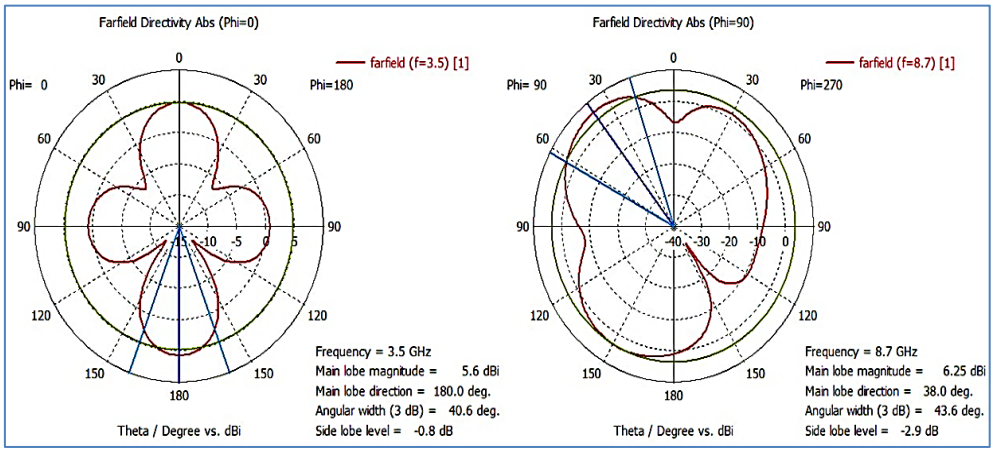

Fig. 9: Radiation pattern as a function of frequency.

CONCLUSION

The design process using CST-2021 simulation software has yielded promising results, indicating that the proposed microstrip patch antenna array is well-suited for a variety of wireless communication applications, including WiMAX and WLAN. The results demonstrate favorable performance across key parameters, consistent with the requirements for efficient and reliable wireless communication systems. Future proposals for improving this design include increasing the array size to (2×2) or (4×4), studying their radiation and optical properties, and designing a compact, high-efficiency dual-band microstrip antenna array using the coaxial cable feeding method.

Conflict of interest: The authors declare no conflicts of interest in relation to this research.

Sources of funding: This research did not receive any specific grant from funding agencies in the public, commercial, or not-for-profit sectors.

Author Contributions: All authors contributed equally to the preparation and completion of this study.

REFERENCES

1. Fang D-G. Antenna theory and microstrip antennas: CRC Press; 2017. https://doi.org/10.1201/b10302

2. Yadav A, Saraswat MK, Palukuru V, Gautam R, editors. Antenna array for 5G C-band for mobile terminals. 2019 TEQIP III Sponsored International Conference on Microwave Integrated Circuits, Photonics and Wireless Networks (IMICPW); 2019: IEEE https://doi.org/10.1109/IMICPW.2019.8933246.

3. Dahake SN, Kolhare NR, editors. Design & development of a 2×2 microstrip patch antenna array in SAR for satellite application. 2017 International Conference on Computing Methodologies and Communication (ICCMC); 2017: IEEE. https://doi.org/10.1109/ICCMC.2017.8282576.

4. Naik PS, Virani H, editors. 1×4 microstrip patch slotted-array antenna for 5G C-band access-point application. 2020 International Conference on Electronics and Sustainable Communication Systems (ICESC); 2020: IEEE. https://doi.org/10.1109/ICESC48915.2020.9156015.

5. Aghoutane B, Das S, El Faylali H, Madhav BTP, El Ghzaoui M, El Alami A. Analysis, design and fabrication of a square slot loaded (SSL) millimeter-wave patch antenna array for 5G applications. Journal of Circuits, Systems and Computers. 2021;30(05):2150086. https://doi.org/10.1142/S0218126621500869

6. Hasan MN, Bashir S, Chu S. Dual-band omnidirectional millimeter wave antenna for 5G communications. Journal of Electromagnetic Waves and Applications. 2019;33(12):1581-90. https://doi.org/10.1080/09205071.2019.1617790.

7. Baza M, Salazar A, Mahmoud M, Abdallah M, Akkaya K, editors. On sharing models instead of data using mimic learning for smart health applications. 2020 IEEE International Conference on Informatics, IoT, and Enabling Technologies (ICIoT); 2020: IEEE. https://doi.org/10.1109/ICIoT48696.2020.9089457

8. Elajoumi S, Tajmouati A, Zbitou J, Errkik A, Sanchez A, Latrach M. Bandwidth enhancement of compact microstrip rectangular antennas for UWB applications. TELKOMNIKA (Telecommunication Computing Electronics and Control). 2019;17(3):1559-68. http://doi.org/10.12928/telkomnika.v17i3.9184.

9. Mesquita MDS, D'Assunção AG, Oliveira JBL, Batista YMV. A new conductive ink for microstrip antenna and bioinspired FSS designs on glass and fiberglass substrates. Journal of Microwaves, Optoelectronics and Electromagnetic Applications. 2019;18:227-45. https://doi.org/10.1590/2179-10742019v18i21554

10. Midasala V, Siddaiah P. Microstrip patch antenna array design to improve gains. Procedia Computer Science. 2016;85:401-9. https://doi.org/10.1016/j.procs.2016.05.181

11. Chater N, Mazri T, Benbrahim M, editors. Design and simulation of a microstrip patch array antenna for electronic-scanning radar application. 2017 International Conference on Wireless Technologies, Embedded and Intelligent Systems (WITS); 2017: IEEE. https://doi.org/10.1109/WITS.2017.7934635

12. Al-Tamimi HM, Nukhailawi YJ, Abdulwahed SH, editors. Design of an elliptical microstrip antenna for multiband wireless signal processing applications. AIP Conference Proceedings; 2023: AIP Publishing. https://doi.org/10.1063/5.0135966.

13. Elkady HM, Abdullah HH, Darwish SM. Multiband circularly polarised CubeSat antenna operating in S, C, X, Ku, K, and Ka bands. IET Microwaves, Antennas & Propagation. 2024;18(2):82-95. https://doi.org/10.1049/mia2.12444

14. Mohammed AS, Alshamri MAA. Design and feed two microstrip antennas with different feed methods and compare their properties. Tikrit Journal of Pure Science. 2024;29(4):52-60. https://doi.org/10.25130/tjps.v29i4.1635

15. Ahmed AA, Alatallah FS, Ali YM. Design of a multiband microstrip patch antenna with bandwidth enhancement for a wireless communication system. Tikrit Journal of Pure Science. 2020;25(4):53-60. . https://dx.doi.org/10.25130/tjps.25.2020.069.

16. Elias, BBQ, Ismail, MM, Alanssari, AI, Rhazali, Z, Soh, PJ, Misran, H, et al. A Metasurface-Based High-Gain Patch Antenna for Future Multiband Wireless Communication. Iraqi Journal of Information and Communication Technology. 2024;7(1):47-60. https://doi.org/10.31987/ijict.7.1.268

17. Abdulhussein A, Khalaf W, Abdulhussein N, Awad EI, Ali AM. Design and Analysis of the Hexagonal-Shaped Antenna with Multiband Features for WLAN, WiMAX, and LTE Applications. Iraqi Journal of Physics. 2023;21(2):33-43. https://doi.org/10.30723/ijp.v21i2.1112.

18. Ali SH, Alfalahi AH, Hachim YA. A Miniaturized Compact Wideband Partial Ground Antenna Used in RFID Systems. Tikrit Journal of Engineering Sciences. 2020;27(2):40-5. http://dx.doi.org/10.25130/tjes.27.2.05.